REFERENCES

[1] J. R. Treichler, I. Fijalkow, and C. R. Johnson, Jr., "Fractionally spaced equalizer. How long should they really be?," *IEEE Signal Processing Mag.*, vol. 13, pp. 65–81, May 1996.

[2] D. N. Godard, "Self-recovering equalization and carrier tracking in two-dimensional data communication systems," *IEEE Trans. Commun.*, vol. COMM-28, pp. 1867–1875, Nov. 1980.

[3] G. J. Foschini, "Equalization without altering or detecting data," *AT&T Tech. J.*, pp. 1885–1911, Oct. 1985.

[4] Z. Ding, R. A. Kennedy, B. D. O. Anderson, and C. R. Johnson, Jr., "Ill-convergence of godard blind equalizers in data communication systems," *IEEE Trans. Commun.*, vol. 39, pp. 1313–1327, Sept. 1991.

[5] Z. Ding, C. R. Johnson, Jr., and R. A. Kennedy, "On the (non)existence of undesirable equilibria of godard equalizers," *IEEE Trans. Signal Processing*, vol. 40, pp. 2425–2432, Oct. 1992.

[6] Y. Li and Z. Ding, "Convergence analysis of finite length blind adaptive equalizers," *IEEE Trans. Signal Processing*, vol. 43, pp. 2120–2129, Sept. 1995.

[7] Y. Li, K. J. R. Liu, and Z. Ding, "Length- and cost-dependent local minima of unconstrained blind channel equalizers," *IEEE Trans. Signal Processing*, vol. 44, pp. 2726–2735, Nov. 1996.

Robustness to Fractionally-Spaced Equalizer Length Using the Constant Modulus Criterion

T. J. Endres, B. D. O. Anderson, C. R. Johnson, Jr., and M. Green

***Abstract*— This correspondence studies robustness properties of the constant modulus (CM) criterion and the constant modulus algorithm (CMA) to the suboptimal but practical situation where the number of fractionally spaced equalizer coefficients is less than what is needed to remove all intersymbol interference (ISI). Hence, there necessarily exists an error in the equalized signal. Relationships between CM and mean squared error cost functions are established.**

***Index Terms*— Adaptive equalizers, adaptive filters, adaptive signal processiing, equalizers.**

I. INTRODUCTION

The constant modulus (CM) criterion and its stochastic gradient descent [the constant modulus algorithm (CMA)] were originally proposed by Godard for QAM signals in [6] and developed independently by Treichler and Agee for FM signals in [11]. CMA resembles the least mean squares (LMS) algorithm in numerous ways without relying on a training signal; therefore, it has seen broad deployment as well as a rich body of (emerging) literature. For example, [4] and [9] show that fractionally spaced CMA exhibits global asymptotic convergence to a setting that is intersymbol interference (ISI) free under a set of conditions. This correspondence studies the robustness properties of fractionally spaced CMA and the CM criterion when all but one of these conditions is satisfied—the so-called length condition. We seek to establish robustness properties for the case where the finite number of fractionally spaced equalizer (FSE) coefficients is less than that needed to remove all the ISI. Hence, there necessarily exists an error in the equalized signal. When this so-called length condition is not satisfied, we describe the deformation of the CM error surface and relate it to the deformation of the mean square error (MSE) surface for multilevel, real, and complex signaling. The analysis presented here can be used with template channel models to guide FSE length selection. Earlier versions of this work can be found in [2] and [3]. In addition, see [10] for baud-spaced results when the length condition is not satisfied.

The sequel is organized as follows. Section II describes the fractionally spaced communication model and CM theory. Section III describes two analysis approaches that decompose the combined channel-equalizer into ISI-free and ISI-rich parts. Section IV uses these two approaches and establishes relationships between CM and MSE cost functions, and Section V contains concluding remarks. The notation follows the convention that vectors (matrices) are designated by lower (upper) case bold letters. $(\cdot)^*$ denotes conjugation, $(\cdot)^T$ denotes transposition, and $(\cdot)^H$ denotes Hermitian transpose.

Manuscript received August 4, 1997; revised February 27, 1998. This work was supported in part by a Hughes Doctoral Fellowship, the National Science Foundation under Grant MIP-9509011, Applied Signal Technology, and the Australian Commonwealth Government under the Cooperative Research Centres Program. The associate editor coordinating the review of this paper and approving it for publication was Prof. Chi Chung Ko.

T. J. Endres is with Sarnoff Digital Communications, Newtown, PA 18940 USA (e-mail: endres@sdcomm.com).

B. D. O. Anderson is with the Research School of Information Sciences and Engineering, The Australian National University, Canberra, Australia (e-mail: brian.anderson@syseng.anu.edu.au).

C. R. Johnson, Jr. is with the School of Electrical Engineering, Cornell University, Ithaca, NY 14853 USA (e-mail: johnson@ee.cornell.edu).

M. Green is with the Department of Engineering, Faculty of Engineering and Information Technology, The Australian National University, Canberra, Australia (e-mail: michael.green@faceng.anu.edu.au).

Publisher Item Identifier S 1053-587X(99)00753-9.

II. FRACTIONALLY SPACED CMA

A. Fractionally Spaced Communication System Model

The communication system considered is a baseband, linear model that samples the received signal at a fraction $(1/L)$ of the baud interval T. We further assume that carrier and baud synchronization are accomplished independently of equalization; the channel is therefore modeled with a time-invariant finite impulse response (FIR) whose coefficients are contained in a length-Q T/L-spaced vector $\mathbf{c} = [c_0 \;\; c_1 \;\; \cdots \;\; c_{Q-1}]^T$. Similarly, the equalizer is described by a length-N T/L-spaced vector of coefficients $\mathbf{f} = [f_0 \;\; f_1 \;\; \cdots \;\; f_{N-1}]^T$.

The T-spaced combined channel-equalizer $\mathbf{h} = \mathbf{C}\mathbf{f}$ is a length-P vector that maps the baud-spaced source sequence $s(k)$ to the baud-spaced equalizer output $y(k)$ by defining the $P \times N$ matrix $\mathbf{C}$ as a block Toeplitz channel convolution matrix. For example, with $L = 2$

$$\underbrace{\begin{bmatrix} h_0 \\ h_1 \\ \vdots \\ h_{P-1} \end{bmatrix}}_{\mathbf{h}} = \underbrace{\begin{bmatrix} c_1 & c_0 & & & & & \\ c_3 & c_2 & c_1 & c_0 & & & \\ \vdots & \vdots & c_3 & c_2 & \ddots & c_1 & c_0 \\ c_{Q-1} & c_{Q-2} & \vdots & \vdots & \ddots & c_3 & c_0 \\ & & c_{Q-1} & c_{Q-2} & \ddots & \vdots & \vdots \\ & & & & & c_{Q-1} & c_{Q-2} \end{bmatrix}}_{\mathbf{C}} \underbrace{\begin{bmatrix} f_0 \\ f_1 \\ \vdots \\ f_{N-1} \end{bmatrix}}_{\mathbf{f}} \tag{1}$$

assumes that the baud instances are coincident with channel coefficients $c_1, c_3, \cdots, c_{Q-1}$. The matrix $\mathbf{C}$ is referred to as the channel convolution matrix associated with channel vector $\mathbf{c}$.

B. Constant Modulus Criterion

The constant modulus (CM) cost function for dispersion of order $p = 2$ in [6] is expressed as

$$J_{CM} = E\{(|y(k)|^2 - \gamma)^2\} \tag{2}$$

where $y(k)$ are the FSE output samples that are coincident with symbol instances, and γ is the CM dispersion constant (or Godard radius) defined as $\gamma = E\{|s(k)|^4\}/E\{|s(k)|^2\}$.

The constant modulus algorithm (CMA) is the stochastic, gradient search rule that descends this cost surface by updating the FSE coefficients (at baud instances) according to

$$\mathbf{f}(k+1) = \mathbf{f}(k) + \mu(\gamma - |y(k)|^2)y(k)\mathbf{r}^*(k) \tag{3}$$

where μ is a small, positive, tunable step size, and $\mathbf{r}(k) = [r(k) \quad r(k-1) \quad r(k-2) \quad \cdots \quad r(k-N+1)]^T$ is a regressor vector of received samples. It is shown in [4] and [9] that under a set of conditions, adapting a FSE using CMA in (3) exhibits global asymptotic convergence to an ISI-free setting; i.e., the asymptotic, combined channel-equalizer response is on average $\mathbf{h} = \mathbf{e}_\delta$, where $\mathbf{e}_\delta$ represents a pure delay and, therefore, contains a single nonzero coefficient of unit value in its $(\delta+1)$st position. The equalizer is said to achieve perfect equalization. The conditions to achieve perfect equalization include a requirement that the equalizer length be sufficiently long, i.e., essentially matching the time span of the channel impulse response. In this perfect case, the global minima settings of the CM cost function equal (within a phase shift) the Wiener or zero-forcing solutions $\mathbf{f}^\dagger = (\mathbf{C}^H\mathbf{C})^{-1}\mathbf{C}^H\mathbf{e}_\delta$ that minimize the MSE cost function for all possible choices of δ (including polarity). We will use this equivalence between the CM minima and Wiener settings to study the deformation of the CM error surface and its relationship to the MSE surface when the number of FSE coefficients is less than that needed to achieve perfect equalization. Our analysis approaches decompose the combined channel-equalizer response (for a FSE that does not satisfy the length constraint) into a part that achieves perfect equalization and one that contributes ISI.

III. Algebraic Analysis Approaches

A. Channel Perturbation

The first approach taken in addressing the robustness of a CM receiver to under modeling is to consider those channel coefficients that are outside the time span of the FSE as channel perturbations in order to study the CM cost incurred from these perturbation coefficients. Let $\mathbf{c} = [c_0 \quad c_1 \quad \cdots \quad c_{Q-1}]^T$ be the length-Q fractionally sampled channel impulse response vector. Define two length-Q vectors $\mathbf{c}_m$ and $\mathbf{c}_p$ such that $\mathbf{c} = \mathbf{c}_m + \mathbf{c}_p$; vector $\mathbf{c}_m$ contains M $(M \le Q)$ consecutive taps of $\mathbf{c}$ in the same positions as they occurred in $\mathbf{c}$ with zeros in the remaining $Q - M$ positions, and vector $\mathbf{c}_p$ contains the $Q - M$ taps of $\mathbf{c}$ that are not in $\mathbf{c}_m$ in the same positions as they occurred in $\mathbf{c}$, with zeros in the remaining M positions as in

$$\mathbf{c}_m := \left[\underbrace{0 \;\; 0 \;\; \cdots \;\; 0}_{\Delta \text{zeros}} \;\; c_\Delta \;\; c_{\Delta+1} \;\; \cdots \;\; c_{\Delta+M-1} \underbrace{0 \;\; 0 \;\; \cdots \;\; 0}_{Q-M-\Delta \text{zeros}}\right]^T$$

$$\mathbf{c}_p := \left[c_0 \;\; c_1 \;\; \cdots \;\; c_{\Delta-1} \underbrace{0 \;\; 0 \;\; \cdots \;\; 0}_{M \text{zeros}} \;\; c_{\Delta+M} \;\; c_{\Delta+M+1} \;\; \cdots \;\; c_{Q-1}\right]^T. \tag{4}$$

Further, let $\mathbf{C}_m$, $\mathbf{C}_p$, and $\mathbf{C}$ be the convolution matrices associated with vectors $\mathbf{c}_m$, $\mathbf{c}_p$, and $\mathbf{c}$, respectively (see Section II-A). The combined channel equalizer can be written as

$$\mathbf{h} = \mathbf{C}\mathbf{f} = \underbrace{\mathbf{C}_m\mathbf{f}}_{\mathbf{h}_m} + \underbrace{\mathbf{C}_p\mathbf{f}}_{\mathbf{h}_p}. \tag{5}$$

By choosing $\mathbf{f}$ as a Wiener setting for channel $\mathbf{c}_m$, which achieves perfect equalization, vector $\mathbf{h}_m = \mathbf{C}_m\mathbf{f}$ contributes no error to the equalized signal. Vector $\mathbf{h}_p = \mathbf{C}_p\mathbf{f}$, however, is the effect of channel perturbations outside the FSE time span and contributes error to the equalized signal.

B. Equalizer Truncation

A related approach to that above is to consider the effect of discarding equalizer coefficients from the ISI-free setting. With a few new definitions, the combined channel-equalizer response can be decomposed into a term that achieves perfect equalization and one that contributes ISI due to violation of the length condition, as in (5). Let $\mathbf{f}^\dagger = [f_0^\dagger \;\; f_1^\dagger \;\; \cdots \;\; f_{N-1}^\dagger]^T$ be an ISI-free setting for channel $\mathbf{c}$, which is of sufficient length to achieve perfect equalization. Define two length-N vectors $\mathbf{f_t}$ and $\tilde{\mathbf{f}}$ such that $\mathbf{f_t} = \mathbf{f}^\dagger + \tilde{\mathbf{f}}$; vector $\mathbf{f_t}$ contains M coefficients of $\mathbf{f}^\dagger$ in the same positions as they occurred in $\mathbf{f}^\dagger$ with zeros in the remaining $N - M$ positions, and vector $-\tilde{\mathbf{f}}$ contains the $N-M$ taps of $\mathbf{f}^\dagger$ that are not in $\mathbf{f_t}$ in the same positions as they occurred in $\mathbf{f}^\dagger$ with zeros in the remaining M positions. For example, one such partitioning is

$$\mathbf{f_t} := \left[f_0^\dagger \;\; f_1^\dagger \;\; \cdots \;\; f_{M-1}^\dagger \underbrace{0 \;\; 0 \;\; \cdots \;\; 0}_{N-M \; zeros}\right]^T$$

$$\tilde{\mathbf{f}} := \left[\underbrace{0 \;\; 0 \;\; \cdots \;\; 0}_{M \; zeros} \;\; -f_M^\dagger \;\; -f_{M+1}^\dagger \;\; \cdots \;\; -f_{N-1}^\dagger\right]^T. \tag{6}$$

The combined channel-equalizer response for the truncated equalizer $\mathbf{f_t}$ can be written as

$$\mathbf{h} = \mathbf{C}\mathbf{f_t} = \underbrace{\mathbf{C}\mathbf{f}^\dagger}_{\mathbf{h}_m} + \underbrace{\mathbf{C}\tilde{\mathbf{f}}}_{\mathbf{h}_p}. \tag{7}$$

The vector $\mathbf{h}_m$ is redefined from the approach in Section III-A as $\mathbf{h}_m = \mathbf{C}\mathbf{f}^\dagger$, and this vector is still ISI-free. Similarly, vector $\mathbf{h}_p$ is redefined from the previous section as $\mathbf{h}_p = \mathbf{C}\tilde{\mathbf{f}}$, and it contributes ISI to the combined channel-equalizer $\mathbf{h}$.

Our goal is to determine the effect of $\mathbf{h}_p$ in (5) and (7) on the CM cost function by exploiting the fact that $\mathbf{h}_m$ in (5) and (7) are ISI-free. Recognize that neither $\mathbf{f}$ nor $\mathbf{f_t}$ are length-constrained CM minima for channel $\mathbf{c}$. Thus, $\mathbf{f}$ or $\mathbf{f_t}$ can serve as an upper bound in a performance sense for the optimal solution of any cost function. We will compare the CM and MSE cost functions.

IV. Undermodeled CM and MSE Cost Functions

Using the approaches from Section III, the combined channel-equalizer response for an under modeled FSE is written as $\mathbf{h} = \mathbf{h}_m + \mathbf{h}_p$, where $\mathbf{h}_m$ is ISI-free, and $\mathbf{h}_p$ is not ISI-free. Since the CM global minima are equivalent to the Wiener settings within a phase shift, the coefficients of $\mathbf{h}_m$ can be written as

$$m_i = \begin{cases} e^{j\theta}, & i = \delta \\ 0, & i \neq \delta \end{cases} \tag{8}$$

where θ is an arbitrary phase shift due to the CM criterion's phase insensitivity. [Observe that y and $ye^{j\theta}$ give the same CM cost in (2).] Similarly, define p_i as the coefficients of vector $\mathbf{h}_p$ or $p_i \in \mathbf{h}_p$. Note

that $p_\delta = 0$ by construction for the channel perturbation approach described in Section III-A, as long as N is the minimum length that achieves perfect equalization for the length-M channel $\mathbf{c}_m$. In general, however, $p_\delta \neq 0$ for the equalizer truncation approach described in Section III-B. We next describe the effect of the p_i on the CM cost function by using (8) and the decomposition $h_i = m_i + p_i$, where $h_i \in \mathbf{h}$. The change in CM cost from a perfect setting is calculated as $\Delta J_{\mathrm{CM}} = J_{\mathrm{CM}|\mathbf{h}=\mathbf{h}_m+\mathbf{h}_p} - J_{\mathrm{CM}|\mathbf{h}=\mathbf{e}_\delta}$, where $J_{\mathrm{CM}|\mathbf{h}=\mathbf{e}_\delta} = (\sigma_s^2)^2(\kappa_s^2 - \kappa_s)$ is the CM cost at a global, ISI-free setting that is nonzero for multilevel signaling. The normalized source kurtosis is $\kappa_s = E\{|s|^4\}/(\sigma_s^2)^2$ and is a measure of source "compactness," and σ_s^2 is the source variance. This analysis is written out for PAM signaling, and the result for QAM signaling is then presented without derivation but follows in an analogous manner to the PAM derivation.

A. Deformation of CM Cost Function

The CM cost function for a white, equiprobable PAM source sequence can be expanded from the form in (2) and written in terms of the combined channel-equalizer response as (see [7] or [8])

$$J_{\mathrm{CM}|\mathrm{PAM}} = (\sigma_s^2)^2\left(\kappa_s^2 - 2\kappa_s\sum_{i=0}^{P-1}h_i^2 + \kappa_s\sum_{i=0}^{P-1}h_i^4 + 3\sum_{i=0}^{P-1}\sum_{l=0,\,l\neq i}^{P-1}h_i^2h_l^2\right). \tag{9}$$

We will use the relation $h_i = m_i + p_i$ and set $\theta = 0$ in (8) to reflect a real signal source and real signal processing at the receiver. Hence, $m_i = 1$ for $i = \delta$ and $m_i = 0\ \forall i \neq \delta$.[1]

Consider three terms of (9) separately. The second central moment can be written as

$$\sum_{i=0}^{P-1}h_i^2 = \sum_{i=0}^{P-1}(m_i + p_i)^2 = 1 + 2p_\delta + \sum_{i=0}^{P-1}p_i^2. \tag{10}$$

Similarly, for the fourth central moment

$$\sum_{i=0}^{P-1}h_i^4 = 1 + 4p_\delta + 6p_\delta^2 + 4p_\delta^3 + \sum_{i=0}^{P-1}p_i^4. \tag{11}$$

In addiiton, for the double sum in (9)

$$\sum_{i=0}^{P-1}\sum_{l=0,\,l\neq i}^{P-1}h_i^2h_l^2 = 2(1+2p_\delta)\sum_{i=0,\,i\neq\delta}^{P-1}p_i^2 + \sum_{i=0}^{P-1}\sum_{l=0,\,l\neq i}^{P-1}p_i^2p_l^2. \tag{12}$$

Now, collecting terms (10)–(12) and substituting into (9) to form $J_{\mathrm{CM}|\mathrm{PAM}|\mathbf{h}=\mathbf{h}_m+\mathbf{h}_p}$, the CM cost incurred from an under modeled FSE is upper bounded due to optimality by $\Delta J_{\mathrm{CM}|\mathrm{PAM}} = J_{\mathrm{CM}|\mathrm{PAM}|\mathbf{h}=\mathbf{h}_m+\mathbf{h}_p} - J_{\mathrm{CM}|\mathrm{PAM}|\mathbf{h}=\mathbf{e}_\delta}$, or

$$\begin{aligned}\Delta J_{\mathrm{CM}|\mathrm{PAM}} = {} & \left[4\kappa_s(\sigma_s^2)^2p_\delta^2 + (\sigma_s^2)^2(6-2\kappa_s)\sum_{i=0,\,i\neq\delta}^{P-1}p_i^2\right] \\ & + p_\delta\left[4\kappa_s(\sigma_s^2)^2p_\delta^2 + 12(\sigma_s^2)^2\sum_{i=0,\,i\neq\delta}^{P-1}p_i^2\right] \\ & + \left[\kappa_s(\sigma_s^2)^2\sum_{i=0}^{P-1}p_i^4 + 3(\sigma_s^2)^2\sum_{i=0}^{P-1}\sum_{l=0,\,l\neq i}^{P-1}p_i^2p_l^2\right].\end{aligned} \tag{13}$$

[1]The case where $\theta = \pi$ (or $m_\delta = -1$) is shown to be equivalent in [1].

The analogous result for QAM signaling with a complex receiver is

$$\begin{aligned}\Delta J_{\mathrm{CM}|\mathrm{QAM}} = {} & \left[\kappa_s(\sigma_s^2)^2(p_\delta^2e^{-2j\theta} + (p_\delta^*)^2e^{2j\theta} + 4|p_\delta|^2)\right. \\ & \left. + \sum_{i=0,\,i\neq\delta}^{P-1}|p_i|^2\left((\sigma_s^2)^2(4-2\kappa_s)\right)\right] + (p_\delta^*e^{j\theta} + p_\delta e^{-j\theta}) \\ & \cdot\left[2\kappa_s(\sigma_s^2)^2|p_\delta|^2 + 4(\sigma_s^2)^2\sum_{i=0,\,i\neq\delta}^{P-1}|p_i|^2\right] \\ & + \left[\kappa_s(\sigma_s^2)^2\sum_{i=0}^{P-1}|p_i|^4 + 2(\sigma_s^2)^2\sum_{i=0}^{P-1}\sum_{l=0,\,l\neq i}^{P-1}|p_i|^2|p_l|^2\right].\end{aligned} \tag{14}$$

Observe that (13) and (14) are grouped according to powers of the perturbation elements p_i, and each contains quadratic, cubic, and quartic contributions. We next perform a similar analysis on the MSE cost function and relate (13) and (14) to the MSE cost incurred due to under modeling.

B. Relation to MSE

In order to compare the deformations of the CM and MSE cost functions due to an under-modeled FSE, the MSE cost function for a white, zero-mean, equiprobable source sequence is expressed as

$$\begin{aligned}J_{\mathrm{MSE}} &= E\{|y(k) - s(k-\delta)|^2\} \\ &= \sigma_s^2\left(\sum_{i=0}^{P-1}|h_i|^2 - h_\delta^* - h_\delta + 1\right).\end{aligned} \tag{15}$$

Now, letting $h_i = m_i + p_i$ with $\theta = 0$ in (8) implies that the MSE cost changes from zero to

$$\Delta J_{\mathrm{MSE}} = \sigma_s^2\sum_{i=0}^{P-1}|p_i|^2. \tag{16}$$

Compare (16) with (13) and (14); when the p_i are small (for example, from small equalizer coefficients, which are neglected (see Section III-A) or from small channel perturbations outside the FSE time span (see Section III-B), the cubic and quartic contributions of (13) and (14) are negligible, and the quadratic terms dominate. In this case, the CM cost incurred is approximately a scaled version of the MSE cost incurred. Defining κ_g as the kurtosis of a Gaussian source distribution (which equals 3 for real signaling and 2 for complex signaling), this relation between the deformations in the CM and MSE cost functions is expressed as

$$\Delta J_{\mathrm{CM}} \approx 2\sigma_s^2(\kappa_g - \kappa_s)\cdot\Delta J_{\mathrm{MSE}}. \tag{17}$$

In this case, the MSE of the under-modeled CM receiver may be approximately upper bounded by $(2\sigma_s^2(\kappa_g - \kappa_s))^{-1}\cdot\Delta J_{\mathrm{CM}}$, where ΔJ_{CM} is calculated according to (13) or (14). Fig. 1 uses the $T/2$-spaced, microwave channel model designated as channel 3 of the SPIB database at http://spib.rice.edu with 16-QAM signaling. The top plot is the channel impulse response magnitudes. The middle plot corresponds to the channel perturbation approach described in Section III-A, whereas the lower plot corresponds to the equalizer truncation approach described in Section III-B. The solid line in these plots is $(2\sigma_s^2(\kappa_g - \kappa_s))^{-1}\cdot\Delta J_{\mathrm{CM}}$, and the dotted line is the MSE in (16) both versus FSE length. The line of constant MSE is a threshold for which CMA is transferred to a decision directed (DD) algorithm, which corresponds to a symbol error rate between 10^{-1} and 10^{-2} for 16-QAM. Observe that far fewer FSE coefficients are needed to reach this threshold than are needed for perfect equalization. For both analysis approaches, the dashed and dotted lines become inseparable

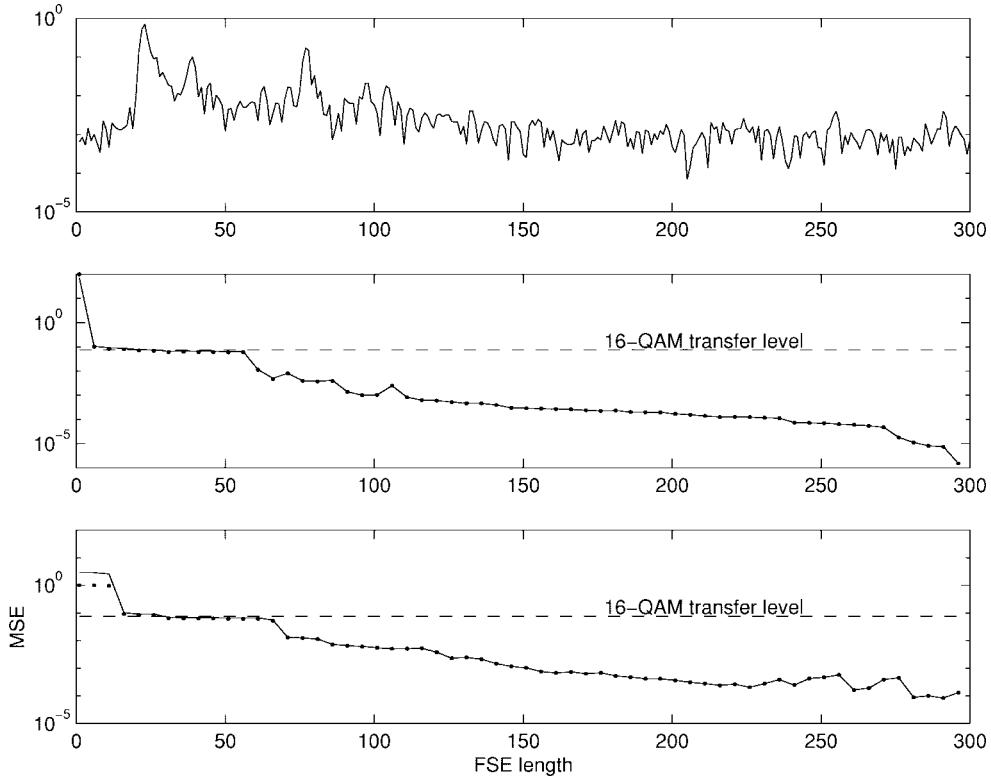

Fig. 1. Top plot is the channel impulse response magnitudes, middle plot is MSE of CM (solid) and MSE (dotted) versus FSE length for the analysis approach in Section III-A, and bottom plot is the same for the approach in Section III-B.

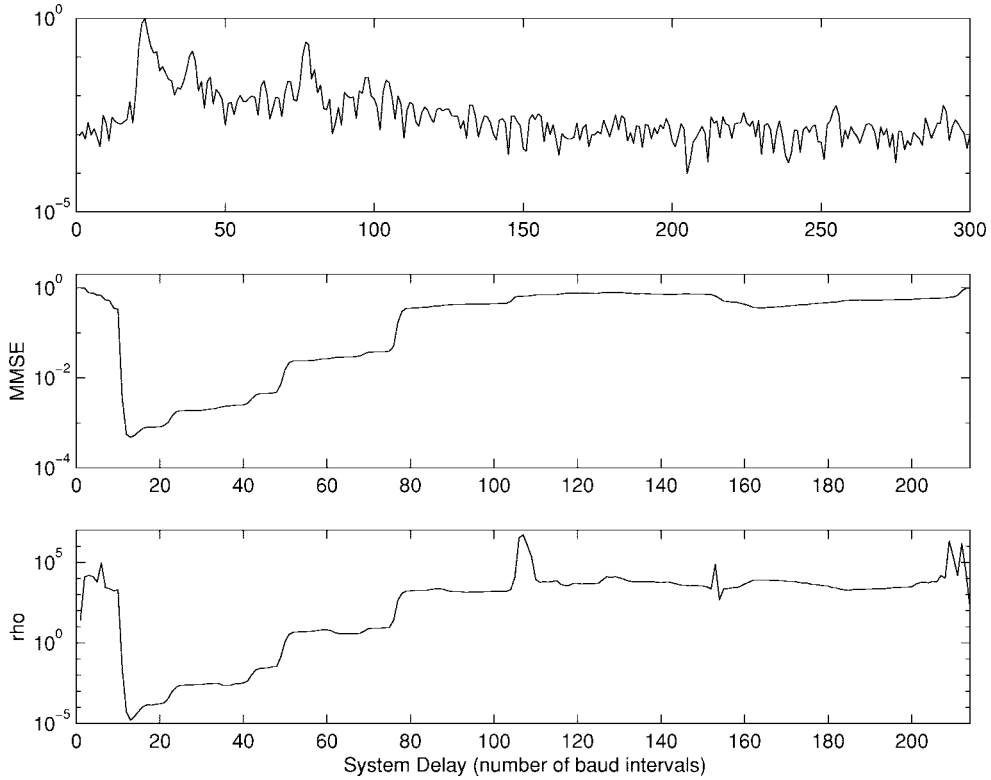

Fig. 2. Top plot is the channel impulse response magnitudes, middle plot is the MMSE versus system delay, and bottom plot evaluates ρ, which is a measure of CM and Wiener minimum proximity for all possible system delays.

when they are less than this threshold. Results for other database channels look similar. This behavior suggests a small deformation in both error surfaces due to under modeling so that the CM minimum stays in a tight neighborhood of the Wiener solution. In each of these plots, the system delay chosen is the one that minimizes the MSE.

C. System Delay Dependence

It is well established that the system delay δ in the combined channel-equalizer can influence MSE performance with variations of several orders of magnitude being typical. We now study the effects of system delay on the CM cost function by describing the relative depth between CM local minima associated with different system delays and approximating these local minima settings for the specific case of BPSK signaling.

1) Relative Depth of CM Local Minima: For the equalizer truncation approach in Section III-B, the coefficient p_δ is, in general, nonzero. Notice that (13) and (14) are grouped according to the power of the p_i and that the cubic contributions are proportional to p_δ. This proportionality can be interpreted as indicating the relative depth between CM local minima. For example, when the p_i are, in general, small and the quadratic contributions are similar for different system delays, it is the differences in the cubic contributions, which are proportional to p_δ, that determine the relative CM and MSE costs for these different delays. This observation may influence equalizer initialization strategies that attempt to start adaptation in the region of convergence of a desirable local minima.

2) Proximity of CM and MSE Local Minima as a Function of δ: Since the CM cost function depends on the fourth-order moment of the equalizer vector, in general, there does not exist a closed-form expression for the CM local minima settings. By approximating the CM cost function with a second-order Taylor series expanded about the length-constrained Wiener settings, a closed-form estimate of the CM local minima can be found. This estimate is of the form of the original length-constrained Wiener setting plus a "perturbation" vector. We use this result to infer performance of the CM local minima for the various system delays.

For noiseless BPSK signaling, the gradient vector of the true CM cost function is the length-M vector whose ith element is $\partial J_{\rm CM}/\partial f_i$ and is calculated in [8] as $\nabla_{\mathbf{f}}(J_{\rm CM}) = \mathbf{C}^T\Lambda\mathbf{h}$, where Λ is the $P\times P$ matrix with main diagonal elements $\Lambda_i = (12\sum_{l=0}^{P-1} h_l^2 - 4 - 8h_i^2)$ and zeros elsewhere. The Hessian matrix is the $M \times M$ matrix whose i, jth element is $\partial^2 J_{\rm CM}/\partial f_i \partial f_j$ and is calculated in [8] as $\mathbf{H}_{\mathbf{f}}(J_{\rm CM}) = \mathbf{C}^T\Psi\mathbf{C}$, where $\Psi = (12\sum_{l=0}^{P-1} h_l^2 - 4)\mathbf{I}_{\mathbf{P}} + 24\mathbf{h}\mathbf{h}^T - 24\,\mathrm{diag}(\mathbf{h}\mathbf{h}^T)$, with $\mathrm{diag}(\cdot)$ extracting the main diagonal from its matrix argument.

Let $\mathbf{f}_\delta^*$ be the length-M Wiener solution for channel $\mathbf{c}$ with system delay δ. Note that $\mathbf{C}\mathbf{f}_\delta^*$ is not ISI-free since M does not satisfy the length condition. The second-order Taylor series expanded about each $\mathbf{f}_\delta^*$ has a unique minimum that serves as an estimate to the true CM local minimum associated with system delay δ. These estimates have the form $\hat{\mathbf{f}}_{\rm CM} = \mathbf{f}_\delta^* + \mathbf{p}$, where $\mathbf{p}$ is the "perturbation vector" $\mathbf{p} = -[\mathbf{H}_{\mathbf{f}}(J_{\rm CM})_{|\mathbf{f}_\delta^*}]^{-1}\cdot\nabla_{\mathbf{f}}(J_{\rm CM})_{|\mathbf{f}_\delta^*}$. This perturbation vector can be used to gauge the proximity of CM and Wiener local minima. For example, $\rho = \mathbf{p}^H\mathbf{p}$ is evaluated for all possible system delays on microwave channel 3 of the SPIB database in Fig. 2 for a $T/2$-spaced equalizer with $M = 128$ coefficients. The top plot shows the magnitude of the channel impulse response coefficients, the middle plot shows the minimum MSE (MMSE)—that associated with $\mathbf{f}_\delta^*$—versus system delay, and the bottom plot shows ρ versus system delay. Results for other database channels look similar. This figure suggests that there exist CM local minima in closer proximity to the better Wiener settings than the worse ones. It also suggests that these better CM local minima exist within a small neighborhood of the better Wiener settings.

V. Conclusion

This correspondence has examined the robustness properties of the fractionally spaced CM criterion to the practical situation where the equalizer length is shorter than that needed to remove all the ISI. Relationships between CM and MSE receivers have been established and evaluated using empirically derived channel models. Our results suggest that there exist CM local minima in close proximity to those MSE local minima that correspond to better-performing system delays. The analysis presented here can be evaluated with template channel models and used in establishing design guidelines for FSE length selection. Our results can be combined with [5], which approximates stochastic jitter of CMA to demonstrate that a longer FSE does not necessarily outperform a shorter FSE (see [3]).

Acknowledgment

The authors would like to thank the anonymous referees for their helpful suggestions.

References

[1] T. J. Endres, "Equalizing with fractionally-spaced constant modulus and second-order-statistics blind receivers," Ph.D. dissertation, Cornell Univ., Ithaca, NY, May 1997.

[2] T. J. Endres, B. D. O. Anderson, C. R. Johnson, Jr., and M. Green, "On the robustness of the fractionally-spaced constant modulus criterion to channel order under modeling—Part I," in *Proc. Signal Process. Adv. Wireless Commun.*, Paris, France, Apr. 16–18, 1997, pp. 37–40.

[3] ——, "On the robustness of the fractionally spaced constant modulus criterion to channel order undermodeling—Part II," in *Proc. Int. Conf. Acoust., Speech Signal Process.*, Munich, Germany, Apr. 20–24, 1997, vol. 5, pp. 3605–3608.

[4] I. Fijalkow, F. L. de Victoria, and C. R. Johnson, Jr., "Adaptive fractionally spaced blind equalization," in *Proc. IEEE Signal Process. Workshop*, Yosemite National Park, CA, Oct. 2–5, 1994, pp. 257–60.

[5] I. Fijalkow, C. E. Manlove, and C. R. Johnson, Jr., "Adaptive fractionally spaced blind CMA equalization: Excess MSE," *IEEE Trans. Signal Processing*, vol. 46, pp. 227–231, Jan. 1998.

[6] D. N. Godard, "Self-recovering equalization and carrier tracking in two-dimensional data communication systems," *IEEE Trans. Commun.*, vol. COMM-28, pp. 1867–1875, Oct. 1980.

[7] C. R. Johnson, Jr., P, Schniter, T. J. Endres, J. D. Behm, D. R. Brown, and R. A. Casas, "Blind equalization using the constant modulus criterion: A review," *Proc. IEEE*, vol. 86, pp. 1927–1950, Oct. 1998.

[8] C. R. Johnson, Jr. and B. D. O. Anderson, "Godard blind equalizer error surface characteristics: White, zero-mean, binary case," *Int. J. Adapt. Contr. Signal Process.*, vol. 9, pp. 301–24, July 1995.

[9] Y. Li and Z. Ding, "Global convergence of fractionally spaced Godard (CMA) adaptive equalizers," *IEEE Trans. Signal Processing*, vol. 44, pp. 818–826, Apr. 1996.

[10] Y. Li and K. J. R. Liu, "Static and dynamic convergence behavior of adaptive blind equalizers," *IEEE Trans. Signal Processing*, vol. 44, pp. 2736–2745, Nov. 1996.

[11] J. R. Treichler and B. G. Agee, "A new approach to multipath correction of constant modulus signals," *IEEE Trans. Acoust., Speech, Signal Processing*, vol. ASSP-31, pp. 459–472, Apr. 1983.